Journal of Optoelectronics and Advanced Materials Vol. 6, No. 2, June 2004, p. 533 - 540

INVITED PAPER

THERMODYNAMIC AND KINETIC ANALYSES OF FORMATION OF AMORPHOUS AND NANOCRYSTALLINE ALLOYS WITH THE AID OF COMPUTER AND DATABASE

A. Takeuchi*, A. Inoue

Institute for Materials Research, Tohoku University, Sendai 980-8577 Japan

Thermodynamic and kinetic simulations were performed to clarify the formations of amorphous and nanocrystalline alloys On the basis of the Miedema's model partially assisted by a database, the amorphous-forming composition region (AFCR) and crystallization temperature (T_x) of the multicomponent amorphous alloys were calculated from thermodynamic approaches. On the other hand, kinetic simulations were performed for Ni-Nb binary eutectic system by the phase field model. The AFCRs calculated for ternary alloy systems containing practically important elements such as Al, Cu, Fe, Ni, Ti agree with the experimental trends. The values of T_x for iron-group-based alloys are calculated with approximate errors of several tens of Kelvin to the experimental data. For $Ni_{62.4}Nb_{37.6}$ alloy, the critical cooling rate (R_c) for formation of amorphous phase and incubation time (τ) for crystallization are calculated to be $R_c = 3\times10^2$ K/s and τ=1000 s. These values are closed to the value calculated from the time-transformation diagram for crystallization based on the homogeneous nucleation theory (R_c=1.4×10^3 K/s τ=10^5 s). The present study indicates the importance of the simultaneous analyses of transformations from thermodynamic and kinetic aspects for the development of amorphous alloys in near future.

(Received April 26, 2004; accepted June 3, 2004)

Keywords: Thermodynamics, Kinetics, Amorphous alloy, Nanocrystalline alloy, Database

1. Introduction

Over the last decade, bulk amorphous alloys with thicknesses of more than a few millimeters have been found in succession in multicomponent alloy systems [1]. The discovery of these bulk amorphous alloys is regarded as an epoch-making incident in the field of non-equilibrium materials because of the significant contributions to widening the scientific and engineering application fields. Almost all of the conventional amorphous alloys were discovered just relying on empirical criteria [1] for the achievement of high glass-forming ability that require us to spend much efforts and working time.

In parallel with the experimental research, computational analyses based on the kinetic or thermodynamic approaches also have been performed separately in order to clarify the essence of the formation and the characteristics of the amorphous alloys. For instance, the former approach performed by molecular dynamics simulation [2] succeeded in proving the necessary conditions for formation of metallic glasses corresponding to the above criteria [1]. On the other hand, the latter approaches [3-4] have been carried out in order to clarify the stability of the amorphous alloys by the construction of time-transformation diagrams. However, in dealing with amorphous alloys computationally, one encounters much difficulty due to the multicomponent effect and the non-equilibrium state. Therefore, the calculations are usually performed for binary systems with a lot of assumptions and approximations.

Besides the above research, database for amorphous alloys has been constructed in a rapid pace throughout the world. For instance, the formations of ternary amorphous alloys are summarized

* Corresponding author: takeuchi@imr.tohoku.ac.jp

as a databook [5] and many kinds of corresponding database are accessible through the internet. Thus, using database efficiently in computations can be another approach for the development of amorphous alloys.

The purposes of the present study is to create a calculation model from the calculation techniques which have been separately developed in the early studies, and to synthesize the kinetic and the thermodynamic calculation models with the help of the database for the development of amorphous alloys.

2. Calculation methods

Thermodynamic calculations were performed on the basis of Miedema's semi-empirical model [6,7] with the help of the database of ternary amorphous alloys [5] whereas kinetic computer simulations were performed by the Phase Field Model that was used for the solidification analyses by Drolet et al. [8].

2.1. Amorphous-forming composition region (AFCR)

By applying Miedema's model, one can calculate amorphous-forming composition region (AFCR). For instance, Murty et al. [9] applied this calculation technique for Cu-Ti base amorphous alloys, and found that the calculation results are in good agreement with the experimental data. The steps of this calculation method are firstly taking two kinds of enthalpies of amorphous ($\Delta H^{\text{amor.}}$) and solid solution ($\Delta H^{\text{s.s.}}$) states, and then evaluating their hierarchy, e.g. an amorphous phase is supposed to form in case of the following relationship: $\Delta H^{\text{amor}} < \Delta H^{\text{s.s.}}$ [6,7]. The definitions of ΔH^{amor} and $\Delta H^{\text{s.s.}}$ are given in Eqs.(1) and (2), respectively, consisting of the chemical mixing enthalpy (ΔH^{chem}) as a common term with the following additional term: topological enthalpy ΔH^{topol} for ΔH^{amor} or elastic enthalpy $\Delta H^{\text{elastic}}$ for $\Delta H^{\text{s.s}}$. The ΔH^{topol} is defined by Eq. (3) which expresses the average of the melting point (T_{m}^{i}) of the constituent element with respect to the composition.

$$\Delta H^{\text{amor.}} = \Delta H^{\text{chem}}(\text{amor.}) + \Delta H^{\text{topol}}, \tag{1}$$

$$\Delta H^{\text{s.s.}} = \Delta H^{\text{chem}}(\text{s.s.}) + \Delta H^{\text{elastic}}, \tag{2}$$

$$\Delta H^{\text{topol}} = 3.5 \sum_{\text{i}=1}^{3} c_{\text{i}} T_{\text{m}}^{\text{i}} . \tag{3}$$

On the other hand, the $\Delta H^{\text{elastic}}$ is calculated by Eshelby's hole and sphere model [10]. In principle, one can calculate AFCR even for the multicomponent systems as long as the constituents elements are from 73 elements which can be dealt with the Miedema's model.

2.2. Crystallization temperature of multicomponent amorphous alloys

One can calculate the crystallization temperature (T_{x}) of binary amorphous alloys [6,7] by applying Miedema's model in the following procedures. First, cavity formation enthalpy (ΔH^{for}) created by a smaller atom in a binary system is calculated. Then, substituting the values of ΔH^{for} into the relationship between T_{x} and ΔH^{for}, $T_{\text{x}} = 5\Delta H^{\text{for}} + 275$, which is obtained by statistical analyses for binary alloys [7]. This calculation method results in a concept that the crystallization of amorphous alloys occurs with motions of atoms through the cavities. This concept is similar to the facts that diffusivity in crystalline alloys is controlled by vacancies, and that the vacancy formation energy acts as an barrier for diffusion of atoms. As for amorphous alloys, atomic diffusion leading to crystallization is thus controlled by the cavities by definition. One of the disadvantages of this calculation method is that the model can deal with the binary systems only. However, we have very recently succeeded in extending the model to multicomponent alloy systems [11]. In our early study, we derived Eq. (4) for the calculations of ΔH^{for} for the multicomponent system with N-component elements

$$\Delta H^{\text{for}} = \left\{ \sum_{i=1}^{N} \sum_{j\neq i,\, j=1}^{N} \left[\left(\mathrm{Ai}_{\mathrm{xi}} + \mathrm{Aj}_{\mathrm{xj}} \right) \Delta H^{\text{for}} \left(\mathrm{Ai}_{\mathrm{xi}} \mathrm{Aj}_{\mathrm{xj}} \right) \right] \right\} - \sum_{j=3}^{N} \sum_{i=1}^{j} \mathrm{x}_i \Delta H^{\text{for}} (\mathrm{Ai}), \quad (4)$$

where $\mathrm{Ai}_{\mathrm{xi}}$ denotes the i-th element having composition of xi with the definitions that A and x stand for the element and its composition, respectively, and that i and j are the symbols to distinguish the elements. It is noted that ΔH^{for} can be calculated for any arbitrary compositions of multicomponent systems. By calculating the values of ΔH^{for} by Eq. (4) and collecting necessary experimental values of T_{x} of multicomponent systems through the database, one can obtain the relationship between T_{x} and ΔH^{for}. The details of the assumptions and approximations made in this calculation method is discussed in the previous paper [11].

2.3. Phase field model (PFM)

The formation and the crystallization processes of amorphous alloys were calculated by referring to the early study of Drolet et al [8] in which PFM was used for the analyses of solidification of a hypothetical binary system. In the present study, the calculation method is improved in order to apply the model to the actual binary alloys by using regular solution model for the descriptions of free energy.

In calculating the kinetics of phase transformation by PFM, conservative and non-conservative parameters are firstly defined, and then they are used for the description of the free energies of the phases. In the present study, the conservative parameter is a composition (c) of the solute element the average of which is constant with respects to time (t) and coordination (x). On the other hand, non-conservative parameter is an order parameter (ψ) which indicates the state of the phase by its sign: liquid or amorphous (ψ<0) or solid (ψ>0) [8]. In the course of the phase transformation, the non-conservative parameter does not hold in a system with progress of time, which enable us to deal with the transformation of the first order.

In describing the free energy, one can use regular solution model as functions of composition and temperature [12]. In the present study, the regular solution model is originally extended by the authors from the conventional one so as to describe the free energy as functions of c, ψ and T shown in Eq. (5):

$$f(c,\psi) = \left\{ \frac{\Omega^{\mathrm{s}} - \Omega^{\mathrm{l}}}{2} \psi + \frac{\Omega^{\mathrm{s}} + \Omega^{\mathrm{l}}}{2} \right\} c(1-c) + RT \sum_{i=1}^{2} c_i \ln c_i + \frac{R}{2} \left(T_{\mathrm{m,A}} - T + \left(T_{\mathrm{m,B}} - T_{\mathrm{m,A}} \right) c \right) (1-\psi) + \left(1-\psi^2\right) \left(\frac{r}{2} - \frac{a}{4} \left(1+\psi^2\right) \right) \quad (5)$$

where Ω^{s} and Ω^{l} are the interaction parameters of solid and liquid phase, respectively, R the gas constant, T the absolute temperature, $T_{\mathrm{m,i}}$ the melting temperature of the constituent element (i=A or B), and r and a constants. The right hand-side of Eq. (5) consists of four terms. The former two terms express the free energy consisting of enthalpy and entropy expressed by regular solution model. It is noted that the first term expresses the enthalpy of solid solution at ψ=1, and that of liquid state at ψ=-1. The third term expresses the difference in free energy between the solid and liquid states, and is assumed that the Richard law, $\Delta H_{\mathrm{m,i}} = RT_{\mathrm{m,i}}$, holds with respect to the heat of fusion ($\Delta H_{\mathrm{m,i}}$) at $T_{\mathrm{m,i}}$. The fourth term is derived under an assumption that free energies between a solid and a liquid state can be described with a formulae of double potential (Landau-Ginzburg) type in a cross-section of $f(c,\psi)$-ψ.

Equation (5) holds only for a homogeneous system in which both c and ψ are unique at any coordinates and time. In reality, one should consider an inhomogeneous system with respect to c and ψ. The free energy for the inhomogeneous system with fluctuations of c and ψ can be written [8] as Eq. (6),

$$F(c,\psi) = \int \left[f(c,\psi) + \frac{K_{\psi}}{2} \left| \vec{\nabla} \psi \right|^2 + \frac{K_c}{2} \left| \vec{\nabla} c \right|^2 \right] d\vec{x}, \quad (6)$$

where K_{ψ} and K_{c} are the gradient energy coefficients for ψ and c, respectively.

The time evolution of ψ and c are separately calculated by Eqs (7) and (8)

$$\frac{\partial \psi}{\partial t}=-\Gamma_{\psi}\frac{\delta F}{\delta \psi}, \tag{7}$$

$$\frac{\partial c}{\partial t}=\Gamma_{c}\nabla^{2}c(1-c)\frac{\delta F}{\delta c}. \tag{8}$$

where Γ_{ψ} and Γ_{c} are the mobility for ψ and c, respectively.

The formulae of Eqs (7) and (8) differ from those used by Drolet et al. [8] in the following two points. First, Drolet et al. introduced a thermal fluctuation term on the right-hand side of Eqs. (7) and (8), respectively; however, these fluctuation terms are ignored in the present study in order to simplify the calculations. This ignorance of the fluctuation terms can be valid by considering the fact that the present calculations for isothermal annealing and quenching have been performed as the spontaneous phase transformation, such as spinodal decomposition, in which the fluctuation terms hardly affect. Accordingly, the authors have succeeded in calculating phase transformation without fluctuation terms as can be seen in Section 3.3. On the contrary, the fluctuation terms are necessary for the phase transformation with considerable barrier, such as nucleation and growth type. Second, the mobility term is defined as $\Gamma_{c}c(1\text{-}c)$ in Eq. (8) whereas Drolet et al deal with this term as a constant. Since the free energy is described by the regular solution model, one should deal the mobility as a function of composition as $\Gamma_{c}c(1\text{-}c)$ in Eq. (8) in order to avoid divergence of the calculations at c=0 and 1 [13]. The time evolution of the parameters ψ and c are calculated step-by-step with appropriate time intervals in a reciprocal space by the corresponding equations of Eqs. (7) and (8), which are obtained using Fourier transformation [13].

The Γ_{c} can be determined from viscosity combined with Stokes-Einstein equation and the relationship for self diffusion in the following three steps. First, the temperature dependence of viscosity is assumed to be expressed by the Vogel-Fulcher-Tammann equation as Eq. (9):

$$\eta=\eta_{0}\exp\left(\frac{B}{T-T_{0}}\right), \tag{9}$$

where η_{0} is the pre-exponential parameter, B the constant, and T_{0} the ideal glass-transition temperature. For instance, the values of η_{0}, B and T_{0} for $Ni_{62.4}Nb_{37.6}$ metallic glass are given [4] as 0.49×10^{5}Pa·s, 5380 K, and 810 K, respectively. Second, the viscosity is converted to the diffusion coefficient (D) with Stokes-Einstein equation expressed as eq. (10);

$$D=\eta_{0}\frac{k_{B}T}{3\pi a_{0}\eta}, \tag{10}$$

where k_{B} is the Boltzmann constant, a_{0} the mean atomic diameter. Third, Γ_{c} can be obtained from a relation between self diffusion coefficient (D) and the mobility (Γ) for pure elements [13] as $D=\Gamma RT$. By combining the three steps, one can obtain the Γ_{c} as a function of temperature ranging from T_{0} to T_{m}. On the contrary, there exist no theoretical equations for obtaining the value of Γ_{ψ}, thus, the value of Γ_{ψ} was determined from the assumption $\Gamma_{c}/\Gamma_{\psi}=10^{20}$. This ratio was selected from the range, $10^{18}\le\Gamma_{c}/\Gamma_{\psi}\le10^{22}$, which enables us to calculate the time evolution of ψ and c without overshooting for calculations.

2.4. Parameters used for calculations

All the parameters required for the thermodynamic calculations are quoted from the literature[6,7]. On the other hand, the calculation conditions for the PFM are summarized in Table 1. In the present study, different values of a and r are used for isothermal annealing and quenching, respectively. The difference in the values of r and a between the isothermal annealing and quenching are interpreted by the thermodynamic finding that the phase diagram for rapid quenching is

somewhat different than the equilibrium one: usually eutectic reaction shifts to lower temperature side when an alloy is quenched.

Table 1 Parameters used for the calculations for Ni-Nb system.

	Γ_ψ	Γ_χ	K_ψ	K_χ	ρ	α	Ω^λ	Ω^σ
	m^2/s		m^4/s				kJ/mol	
Isothermal annealing quenching	10^{-6}	10^{-26}	10^{-21}	10^{-41}	5 1.5	5 1.5	-5	+30

3. Results and discussion

3.1. Amorphous-forming composition region (AFCR)

Fig. 1 shows the calculation results of AFCR for ternary alloy systems containing practically important elements of Al, Cu, Fe, Ni, Ti. The closed circle represents the calculated AFCR whereas the open circle represents the experimental results quoted from a database [5]. As shown in Fig. 1, the calculated AFCRs reproduce experimental trends for these ternary amorphous alloys. Besides these calculation results, the similar calculations were also performed [14] for 351 ternary amorphous alloys listed in the database [5] containing typical amorphous alloys represented by Al-Ni-Zr, B-Fe-Zr, Al-B-Fe, Cu-Mg-Y and Ni-P-Pd alloy systems. It was reported in the early study [14] that calculated AFCRs tend to be greater than the experimental data as a result of a simplification of the present calculation model that only the difference in enthalpy between the amorphous and solid solution phases is taken into account. Furthermore, it was also pointed out [14] that ignoring the presence of intermetallic compounds in the present calculation method can also affect the discrepancy in AFCRs between the calculated and the experimental data. Therefore, further precise predictions of AFCR are expected by adopting additional calculation conditions with keeping the significant advantage of the present calculation model that the AFCRs can be calculated for the multicomponent systems from constituent elements as many as 73 [6,7].

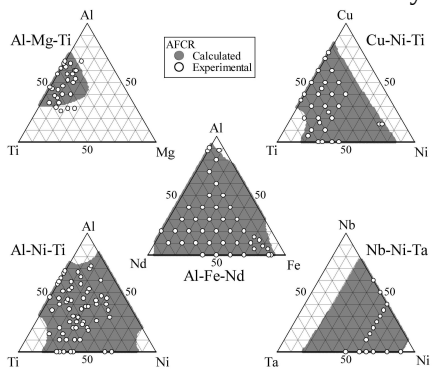

Fig. 1. AFCR calculated for ternary amorphous alloy systems containing practically important elements of Al, Cu, Fe, Ni, Ti.

3.2. Crystallization temperature of multicomponent amorphous alloys

As a result of the statistic analyses of the relationship for the multicomponent systems between the values of experimentally measured T_x listed in the original literatures of the databook [5] and ΔH^{for}, we obtained the following relationship [11]: T_x=4.16ΔH^{for} +318. In the present study, T_x of some iron-group-based, Pd-based and $Ni_{62.4}Nb_{37.6}$ amorphous alloys were calculated and the calculation results are summarized in Table 2.

As shown in Table 2, the values of $T_x^{cal.}$ tend to be greater than those of $T_x^{exp.}$, and the difference in T_x's is greater than 50 K except for the $Ni_{62.4}Nb_{37.6}$ amorphous alloy. Thus, the present

model yields the T_x for iron-group-based amorphous alloys with approximate errors of several tens of Kelvin to the experimental data. The difference in T_x between the calculated and experimental values is somewhat large for using the present calculation method. Accordingly, further improvements of the present model are greatly expected so as to use the present calculation method for the development of new amorphous alloys.

Table 2. Crystallization temperature calculated ($T_x^{cal.}$) and that experimentally obtained ($T_x^{exp.}$).

Alloy	$T_x^{exp.}$ / K	$T_x^{cal.}$ / K	$T_x^{cal.} - T_x^{exp.}$ / K
$Fe_{79}Si_{10}B_{11}$	750	873	123
$Co_{75}Si_{15}B_{10}$	793	866	73
$Ni_{75}Si_8B_{17}$	733	815	82
$Ni_{62.4}Nb_{37.6}$	923	946	23
$Pd_{40}Ni_{40}P_{20}$	724	806	82
$Nd_{60}Fe_{30}Al_{10}$	722	842	120
$Pd_{40}Cu_{30}Ni_{10}P_{20}$	656	722	66

3.3. Formation and crystallization processes of amorphous alloys

Fig. 2 shows the Ni-Nb binary phase diagram used for the calculations. The solid line shows the equilibrium phase diagram quoted from the literature[15] and the broken line shows the calculated phase diagram which was computed by Eq. (5) with the parameters listed in Table 1. The calculated phase diagram shows the hypothetical deep eutectic reaction which can be seen by extrapolation in the equilibrium phase diagram. On the basis of the calculated phase diagram in Fig. 2, the formations of amorphous and crystalline alloys were calculated for the conditions of quenching and isothermal annealing.

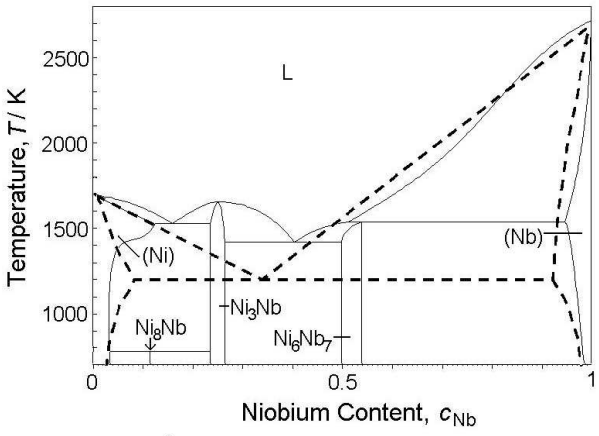

Fig. 2. Equilibrium (solid line) and calculated (broken line) phase diagrams of Ni-Nb binary system.

Fig. 3 shows the calculation results performed with several cooling rates (R) ranging from 3×10^3 to 1×10^{-2} K/s. As shown in Fig. 3(a), the value of ψ tends to increases with decreasing R. This tendency indicates that amorphous phase transforms to crystalline phase, which can be judged from the definition of ψ described in Section 2: liquid(amorphous) (ψ<0) or solid (ψ>0). As can be seen in Fig.3 (a) the values of ψ remain nearly -1 up to R =3×10^2 K/s, indicating that critical cooling rate (R_c) for formation of amorphous phase is approximately R_c =3×10^2 K/s. Then, the value of ψ drastically increases with decreasing R, and reaches ψ >1 at R =3×10^1. This implies that the crystalline phase forms at R =3×10^1 K/s. As shown in Fig. 3(b), however, the composition profile at R =3×10^2 has a small deviations from the average composition, implying that solid solution phase forms at R =3×10^2 K/s. Further decrease in R causes the decomposition of the solid solution, which can be seen in Fig. 3(b) at the cooling rate of R =1×10^{-2} K/s.

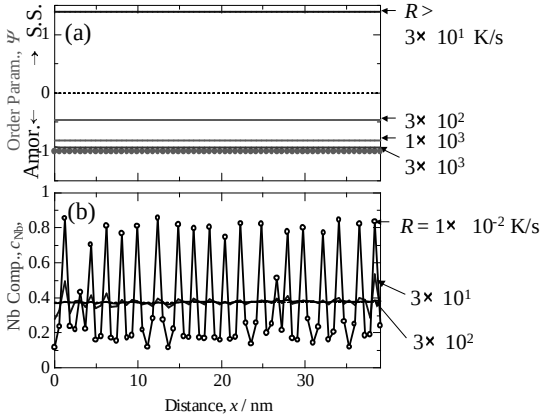

Fig. 3. Amorphous and nanocrystalline alloy formations calculated as a function of cooling rate.

Fig. 4 shows the calculation results isothermally annealed at 960 K. The calculation was performed by applying an initial ψ profiles with an amplitude of 0.5 and wavelength of about 13 nm. As shown in Fig. 4(a), ψ increases keeping wave-profile with increasing time, and then reaches maximum near the value of 1 at t=1000 s. Further annealing leads to the increase of ψ so that ψ reaches ψ =1 at t=10000 s. From these change in ψ, the crystallization starts around t=1000 s, and then completes at t=10000 s. It appears from Fig. 4(b) that decomposition in c starts at t=1000 s. From the calculation results shown in Fig. 4, the incubation time (τ) for crystallization from amorphous phase at T=960 K is estimated to be approximately 1000 s.

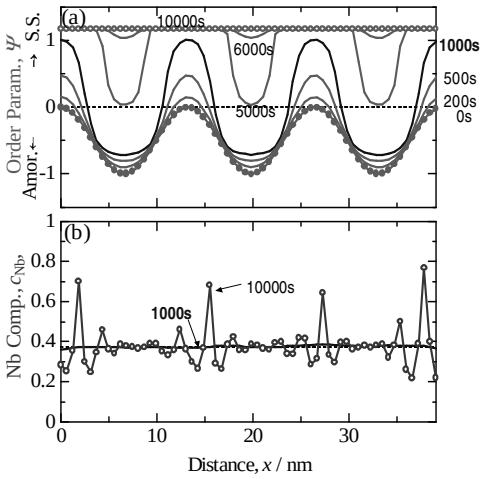

Fig. 4. Calculation results of crystallization process of amorphous phase isothermally annealed at 960 K.

According to thermodynamic approach conducted by Davies [4], R_c for formation of amorphous phase for $Ni_{62.4}Nb_{37.6}$ is calculated to be 1.4×10^3 K/s, and the τ for crystallization at T=960 K can be evaluated to be 10^5 s, the latter of which is calculated from the time-transformation diagram for $Ni_{62.4}Nb_{37.6}$ computed on the basis of the homogeneous nucleation theory [4]. Although the values of R =3×10^2 K/s and τ=1000 s calculated kinetically in the present study are smaller than those values obtained by thermodynamic approaches by a factor of nearly 100, the R_c and τ obtained in the present study are considered to be appropriate judging from the simplification inherent in the present model, e.g. one-dimensional calculation, uncertainties of values of Γ_ψ and the dependence of initial ψ profiles on τ and so on.

4. Conclusions

The thermodynamic calculations based on Miedema's semi-empirical model and the kinetic analyses by phase field model were performed with the help of the experimental data quoted form a database. The AFCR calculated for ternary alloy systems containing practically important elements such as Al, Cu, Fe, Ni, Ti agrees with the experimental trends. The T_x for iron-group-based alloys are calculated with approximate error of several tens of Kelvin to the experimental data. Furthermore, amorphous and nanocrystalline phase formations were performed. For $Ni_{62.4}Nb_{37.6}$ alloy, R_c for formation of amorphous phase and τ for crystallization at T=960 K are calculated to be 3×10^2 K/s and 1000 s, respectively. These values calculated kinetically are smaller than those obtained from thermodynamic analyses based on the homogeneous nucleation theory.

References

[1] A. Inoue, Bulk Amorphous Alloys, Preparation and Fundamental Characteristics, Materials Science Foundations **4,** Eds. M. Magini and F.H. Wöhlbier, Trans Tech Publications, Netherlands (1998).
[2] M. Shimono, H. Onodera, Scripta Mater. **44**, 1595 (2001).
[3] D. R. Uhlmann, J. Non-Cryst. Solids **7**, 337 (1972).
[4] H. A. Davies, Rapid Quenching and Formation of Metallic Glasses, Rapidly Quenched Metals III, **1**, ed. B. Cantor, The Metal Society (1978).
[5] Nonequilibrium Phase Diagrams of Ternary Amorphous Alloys, LB, New Ser., Group III, Condensed, Vol. **37**, Eds. Y. Kawazoe, T. Masumoto, K. Suzuki, A. Inoue, J.- Z. Yu, T. Aihara Jr., T. Nakanomyo, A.P. Tsai, Springer (1997).
[6] F. R. de Boor, R. Boom, W. C. M. Mattens, A. R. Miedema, A. K. Nissen, Cohesion in Metals, ed. F. R. Boer and D. G. Perrifor, Elsevier Science Publishers B.V. (1988).
[7] H. Bakker, Enghalpies in Alloy: Miedema's Semi-Empirical Model, Materials Science Foundations **1**, Eds. M. Magini and F.H. Wöhlbier, Trans Tech Publications, Netherlands (1998).
[8] F. Drolet, K. R. Elder, M. Grant, J. M. Kosterliz, Phys. Rev. **E61**, 6705 (2000).
[9] B. S. Murty, S. Ranganathan, M. M. Rao, Mater. Sci. Eng. **A149**, 231 (1992).
[10] J. D. Eshelby, Solid State Phys. **3**, 79 (1956).
[11] A. Takeuchi, A. Inoue, Mater. Trans., **43**, 2275 (2002).
[12] J. H. Hildebrand, J. Am. Chem. Soc. **51**, 66 (1929).
[13] T. Miyazaki, A. Takeuchi, T. Koyama, T. Kozakai, Mater. Trans., JIM, **32**, 915 (1991).
[14] A. Takeuchi, A. Inoue, Mater. Trans. **42**, 1435 (2001).
[15] Desk Handbook: Phase diagrams for Binary Alloys, Ed. H. Okamoto, ASM International, American Society for Metals (2000).